ELSEVIER

Catalysis Today 50 (1999) 285–298

CATALYSIS TODAY

Use of CeO_2-based oxides in the three-way catalysis

J. Kašpar*, P. Fornasiero, M. Graziani

Dipartimento di Scienze Chimiche, via Giorgieri 1, Università di Trieste, 34127, Trieste, Italy

Abstract

In the present paper the use of CeO_2-based materials in the automotive three-way catalysts (TWCs) is considered. The multiple roles of CeO_2 as a TWC promoter and in particular the oxygen storage/release capacity (OSC) are critically discussed. Attention is focused on the advanced OSC materials containing ZrO_2, which are employed in the last generation of catalytic automotive converters. © 1999 Elsevier Science B.V. All rights reserved.

Keywords: Three-way catalysts; CeO_2; ZrO_2; Oxygen storage capacity (OSC)

1. Introduction

1.1. Historical background

Since the beginning of the 1980s, the use of CeO_2 in the automotive pollution control has become so broad to represent today the most important application of the rare earth oxides. The development of the TWCs was dictated by the need to simultaneously convert the hydrocarbons (HCs), CO and NO_x present in the automotive exhaust to H_2O, CO_2 and N_2. The conventional TWCs employed in the late 1980s mostly contained Rh and Pt as active noble metals and CeO_2 as oxygen storage component. Highest conversion of the pollutants is attained close to the stoichiometric conditions, while excursions to fuel-rich (net reducing) or fuel-poor (net oxidizing) air-to-fuel (A/F) ratios severely decrease the efficiency of the TWCs. Such excursions may represent a serious limitation for a TWC since the A/F significantly oscillates around the stoichiometric value $A/F=14.6$ [1,2]. Addition of CeO_2 limits this disadvantage due to its ability to act as an oxygen buffer by storing/releasing O_2 due to the Ce^{4+}/Ce^{3+} redox couple. With higher OSC of the catalyst, higher conversion efficiency and resistance to thermal aging are generally observed.

The increasing restrictions for the standards for the automotive emissions as reported in Table 1, have set new challenges for the development of the new automotive TWCs. In fact, a major problem of the TWC converters is that significant conversions are attained only at high temperatures (>600 K). As a result, during the cold-start of the engine, the emissions of the pollutants, particularly the HC, are quite high until the converter reaches the operating temperature. Accordingly, inclusion of the cold-start in the engine test and the remarkably low limits required in the near future for the HC emissions demanded for the development of the so-called close coupled catalyst (CCC). These catalysts, being manifold mounted, experience temperatures up to 1273–1373 K, which requires an extremely high thermal resistance.

*Corresponding author. Fax: +39-40-6763903; e-mail: kaspar@dschsun1.univ.trieste.it

0920-5861/99/$ – see front matter © 1999 Elsevier Science B.V. All rights reserved.
PII: S0920-5861(98)00510-0

Table 1
US federal, California and European emission standards in g km^{-1} for gasoline fuelled automobiles (CH_4 is excluded in the US and California standards)

Enactment	CO	HC	NO_x	Comments
US federal				
1987	2.11	0.25	0.62	MT 91, tier 0
1994	2.11	0.16	0.25	MT 94, tier 1
2003	1.06	0.08	0.124	Proposed
California				
TLEV	2.11	0.08	0.25	
LEV	2.11	0.05	0.12	
ULEV	1.06	0.02	0.12	
European Union				
1996/97	2.7	0.341	0.252	Directive 94/12
2000/2001	2.3	0.20	0.15	Proposed
2005/2006	1.0	0.10	0.08	Indicated

In the present paper we will shortly review some of the recent developments of the CeO_2-based materials as TWC promoters, particularly in the CCCs. Attention will be given to the role of ZrO_2 in promoting the thermal stability and the OSC efficiency of the CeO_2. It is not our intention to give a comprehensive review of the CeO_2 system or the TWCs, for which we refer the reader to previous literature [1–8]; rather we will focus some of the peculiar aspects of the CeO_2–ZrO_2 and related systems.

At present CeO_2–ZrO_2 mixed oxides containing TWCs represent the most advanced technology for the development of the CCCs. Even though this technology was first employed by the mid-1990s by some automobile companies [9] (fourth generation TWCs), it has not been openly presented by the catalysts makers/washcoater companies until very recently. Thus, during the third CaPOC[1] meeting held in Brussels in 1994 only one independent academic group reported the effectiveness of ZrO_2 in promoting the OSC of CeO_2, while catalysts manufacturers described non-specified promoters [10]. Only at the CaPOC 4 meeting, held in 1997, the effectiveness of ZrO_2 in stabilising CeO_2 against thermal deactivation was claimed out by the industrial researchers [11]. An entire mini-symposium dedicated to the role of ZrO_2 in catalysis was held at the SAE conference in Detroit in February 1997 [12]. Accordingly, the data reported in scientific literature are rather scarce, most of the papers treating this issue appeared in commercial journals. These materials represent today's TWC technology, however, there is a number of open issues to be addressed by the researcher in order to understand the origin of their improved performances compared to the traditional CeO_2-based technology. Further, nowadays, due to future restriction in the exhaust emissions all over the world, it is imperative to further improve their performances and to develop the year's 2005 technology.

2. Role of CeO_2 in the TWCs

It is an ambitious task to define the role of the CeO_2 in the three-way catalysis since multiple effects have been attributed to this promoter [8]. Ceria was suggested to:

- promote the noble metal dispersion;
- increase the thermal stability of the Al_2O_3 support;
- promote the water gas shift (WGS) and steam reforming reactions;
- favour catalytic activity at the interfacial metal–support sites, etc.;
- promote CO removal through oxidation employing a lattice oxygen;
- store and release oxygen under, respectively, lean and rich conditions.

There have been strong discussions on which is the most important promoting effect, argument favouring WGS or OSC have been reported. Whatever is the critical role of CeO_2, as recently pointed out by Robert McCabe, there is certainly a general agreement that "CeO_2 is good!".[2]

A perusal of the above listed effects suggests, however, that there is a common point in all these properties which is related to the ability of NM/CeO_2 system to promote migration/exchange of oxygen species in the reaction. This effect is clearly detected

[1]The symposium on "Catalysis and automotive pollution control" (CaPOC) was held in Brussels every four years since 1986.

[2]Robert McCabe, Plenary Lecture, Proceedings of the Third International Conference on f Elements, Paris, France, September 1997.

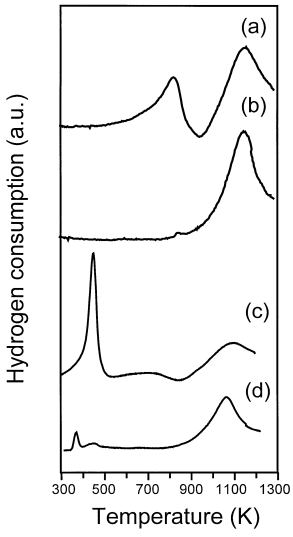

Fig. 1. Temperature programmed reduction of CeO_2 and Rh/CeO_2 and the effects of redox ageing: (a) CeO_2 (194 $m^2\,g^{-1}$); (b) sample from run (a) and oxidised at 700 K (<10 $m^2\,g^{-1}$); (c) Rh/CeO_2 (194 $m^2\,g^{-1}$); (d) sample from run (c) and oxidised at 700 K (<10 $m^2\,g^{-1}$) [19].

when the redox properties, e.g. the oxygen storage, are tested by means of the temperature-programmed reduction (TPR). As shown in Fig. 1, the TPR profile of the high surface area CeO_2 shows the well-known two peaks profile associated with, respectively, reduction at the surface and in the bulk of CeO_2 [13,14]. The presence of rhodium clearly promotes the reduction of the surface oxygen species as documented by the shift of the peak at 770 below 500 K, i.e. at a temperature where reduction of the noble metal oxide precursor occurs. This phenomenon has been attributed to the ability of the noble metal to promote the reduction of CeO_2 via spilling of hydrogen species over the support [13,15–17]. The low temperature reduction is strictly related to the extent of surface area since when a second TPR is performed after an oxidation of the reduced moieties, negligible peaks are observed below 700 K (Fig. 1). In fact, under reducing conditions the CeO_2 surface is poorly stable [18], leading to a surface area collapse in the course of the initial TPR experiment [19]. This results in loss of metal–CeO_2 interactions as detected by the low temperature TPR peak.

The correlation between the low temperature reduction peaks in the TPR profile and the three-way activity appears now well established for the CeO_2-based catalysts. The thermal ageing leads to loss of noble metal–CeO_2 interactions as detected by TPR and simultaneously a significant deactivation of the catalysts is observed (Fig. 2). Also worth noting is that the deactivation seems to be related to two different phenomena: (i) sintering on the noble metal particles leading to a loss of metal surface area; (ii) loss of CeO_2 surface area leading to a loss of the OSC. It is conceivable that the loss of metal surface area leads to a monotonic decrease of activity which indicates that the shadowed area shown in Fig. 2 is attributable to a high OSC in the fresh catalyst.

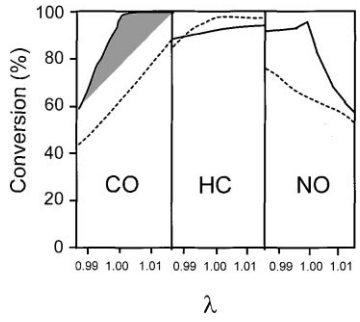

Fig. 2. Effects of thermal ageing at 1173 K on CO, HC and NO_x conversion on $Rh/CeO_2/Al_2O_3$ catalysts during cycled sweep test; (———) fresh, (- - -) aged, GHSV 65 000 h^{-1}, reaction temperature 823 K, dashed area: see text [20].

In summary, it appears that whatever is the true nature of the CeO_2 promotion effects in the TWCs, these effects are noticeable as long as a high surface area, and consequently low temperature reduction features are present in the CeO_2-based catalysts. Accordingly, the research activity in the 1990s has been focussed mainly on the improvement of the surface area stability in the CeO_2 promoter. Among different systems tested, ZrO_2 appeared to be the most effective thermal stabiliser of CeO_2, particularly when it forms a mixed oxide with ceria [9,21]. This system is discussed in the following sections.

2.1. *Synthesis and phase diagram of CeO_2–ZrO_2 mixed oxides*

Before entering into the details of the advanced properties of the CeO_2–ZrO_2 mixed oxides compared to the CeO_2-based TWC technology it is worth to briefly discuss the appearance of the CeO_2–ZrO_2 phase diagram. The CeO_2–ZrO_2 has long been inves-

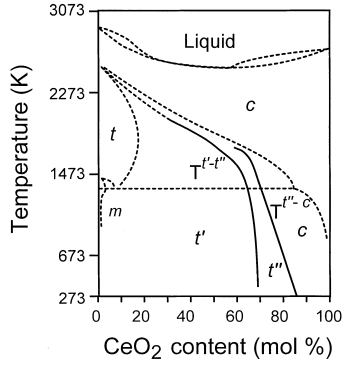

Fig. 3. Phase diagram of the CeO_2–ZrO_2 system [25,27,28].

tigated due to its importance in the field of ceramics and as solid state electrolytes. The exact appearance of this diagram is still a matter of debate despite extensive work of several research groups [22–32]. The main reason is that besides the thermodynamically stable phases, a number of metastable phases have been reported in the literature. As shown in Fig. 3, below 1273 K the phase diagram shows a monophase region of monoclinic (*m*) symmetry for CeO_2 molar contents less than ≈10%, while for CeO_2 contents higher than 80% cubic (*c*) phase was reported [32,33]. In the intermediate region, the true nature of CeO_2–ZrO_2 phase diagram is still unclear. In this region indeed a number of stable and metastable phases of tetragonal symmetry are observed [30,34,35]. According to Yashima et al. [25,27,28] three different *t*, *t′* and *t″* phases can be distinguished on the basis of XRD and Raman characterisation. Of these, the *t*-form is a stable one formed through a diffusional phase decomposition, the *t′*-form is obtained through a diffusionless transition and it is metastable, while the *t″*-form is an intermediate between *t′* and *c*. It shows no tetragonality and it exhibits an oxygen displacement from ideal fluorite sites. The *t″* phase is often referred to as a *cubic* phase because its XRD pattern is indexed in the cubic Fm3m space group [36]. This is due to the fact that the cation sublattice prevalently generates the XRD pattern. For the sake of clarity, the characteristics of all the phases are summarised in Table 2.

The phase boundaries as indicated in Fig. 3 should be considered very approximate due to the fact that in the case of the metastable tetragonal phases, the kind of distortion from the fluorite type structure is highly sensitive to the particle size. Thus Yashima et al. observed that the *t″* phase is formed for CeO_2 contents above 65 mol%, while we reported the formation of the same phase for a $Ce_{0.5}Zr_{0.5}O_2$ sample [36]. The reasons for such apparent discrepancies can be rationalised by analogy with pure ZrO_2. In fact, at room temperature (rt) the *m*-ZrO_2 is the thermodynamically stable phase, however, either tetragonal or cubic ZrO_2 have been stabilised at rt provided that fine particles are formed in the synthesis. Different explanations have been advanced to account for the stabilisation of *t*-ZrO_2: surface and strain energy effects [37–39]; strain energy effects generated at domain boundary [40]; structural similarity [41] and/or topotactic crystallisation [42] of *t*-ZrO_2 from the amorphous phase. The latter two explanations are rather kinetic than thermodynamic. Nevertheless, all these investigations point out that below a critical crystallite size, the tetragonal phase is favoured over the monoclinic one. Consistently, by using extremely fine particles, even the *c*-ZrO_2 was stabilised at rt [43–45].

In addition to the above considerations, one should note that specific compounds have also been proposed

Table 2
Classification of the phases in the CeO_2–ZrO_2 binary system[a]

Phase	Composition range (mol% Ce)	Tetragonality[b]	Space group
Monoclinic (*m*)	0–10	–	$P2_1/c$
Tetragonal (*t*)	10–30	>1	$P4_2/nmc$
Tetragonal (*t′*)	30–65	>1	$P4_2/nmc$
Tetragonal (*t″*)[c]	65–80	1	$P4_2/nmc$
cubic (*c*)	80–100	1	Fm3m

[a]The classification here reported follows that proposed in [25]. The *t* and *t′* phases correspond to the *TZ°* and *TZ′* phases previously reported by Meriani et al. [31,35].
[b]Defined as axial ratio *c*/*a*.
[c]As written in the text, on the basis of the XRD pattern this phase is commonly indexed in the Fm3m space group [31,35].

to exist in the CeO_2–ZrO_2 system: tetragonal $Ce_2Zr_3O_{10}$ [46] and cubic Ce_3ZrO_8 [47,48]. The existence of the former compound, however, has not been confirmed [32]. Finally, in the discussion of the features of the CeO_2–ZrO_2 phase diagrams, it must be considered that upon reduction of the CeO_2–ZrO_2 mixed oxides a still different situation is observed [49] and the presence of different phases was inferred [50].

The presence of metastable phases in the phase diagram immediately points out the critical importance of the method of synthesis of the mixed oxides and the relevance of the kinetic lability/inertness towards phase separation. As will be shown in the following sections, the homogeneity of a CeO_2–ZrO_2 critically affects both the redox and textural properties. Generally speaking, the Vegard law is widely employed by the researchers to assess the presence of a solid solution. Due to the different ionic radii of Ce^{4+} (0.97 nm) and Zr^{4+} (0.84 nm) [51–53], a linear relationship between the cell parameter and the ZrO_2 content is expected for the cubic samples. Due to the variable *c*/*a* ratio, in the tetragonal region this relationship is related to the cell volume rather than to a single cell parameter. A number of semi- or empirical models have been reported to quantitatively evaluate this variation of the cell parameter [54–57]. In fact, as shown in Fig. 4, several authors experimentally found rather good linear relationships, however, the comparison between the different researchers and even within the same laboratory, when different synthesis methods

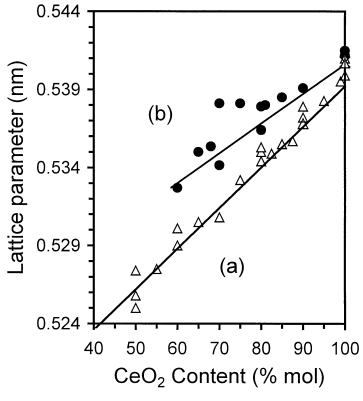

Fig. 4. Experimental lattice parameters reported for the CeO_2–ZrO_2 mixed oxides: (a) low surface area ceramic materials, (b) high surface area materials [58–62].

are employed [58,59], leads to a significant disagreement in the data. Also, the presence of a solid solution is often found only in a limited range of compositions as denoted by a constant lattice parameter in the data taken from Ozawa et al. [60] (Fig. 4).

As shown in Fig. 4, the model reported in [56] fits fairly well the cell parameters reported for ceramic type of CeO_2–ZrO_2 solid solutions, e.g. dense materials with low surface areas. This model has been derived from data reported in [32,63,64], which have not been reported in Fig. 4 but obviously they well fit the model [56]. In contrast, the lattice parameters of the high surface area samples, which were prepared by co-precipitation [59,60] or co-impregnation on Al_2O_3 [65], are significantly higher.

Finally it is worth recalling that a number of different synthetic methods have been applied to prepare CeO_2–ZrO_2 and related mixed oxides: solid state synthesis [66,67]; co-precipitation [59,60,68,69], high energy ball-milling [58,70,71], use of different additives/gelification agents such as hydrazine [48], oxalic acid [61,72,73], citric acid [74,75], sol–gel methods using alkoxide precursors [76–78], formation of aerogels by supercritical drying of hydrogels [79].

2.1.1. *Thermal stability*

The thermal stability of CeO_2 is a critical point in determining the promoting effects of CeO_2. As soon as significant sintering of CeO_2 particles occurs, both OSC and metal–support interactions appear inhibited. The industrial research has spent significant efforts on finding the solution for improving the thermal stability both by modification of the CeO_2 synthesis and by looking for different types of promoters and stabilisers. Use of ZrO_2 resulted in effectively improving the thermal stability of CeO_2 as reported in patent literature [21]. Generally speaking, in these early reports the addition of ZrO_2 was made in an uncontrolled way, mostly by impregnation, and no characterisation of the obtained phases was reported. Further work suggested that the appropriate way of adding ZrO_2 is that of forming a solid solution between the CeO_2 and ZrO_2. Since the early 1990s, evidence has been reported in the open literature concerning the use of CeO_2–ZrO_2 mixed oxides in problems concerning the effectiveness of structural doping of CeO_2 with ZrO_2 in improving the redox and catalytic properties of CeO_2 [60,66,69,80].

The effects of foreign cation doping, at relatively low concentrations (0.5–10 mol%), on the thermal stability of CeO_2 has been extensively investigated by Pijolat et al. [50,81–84]. They tried to rationalise the ability of foreign cations to stabilise CeO_2 against sintering by developing a complete set of equations based on the diffusion of cerium vacancies as the rate limiting step in the sintering process. Among the different cations investigated (Th^{4+}, Zr^{4+}, Si^{4+}, La^{3+}, Y^{3+}, Sc^{3+}, Al^{3+}, Ca^{2+}, and Mg^{2+}), those with ionic radii smaller than that of Ce^{4+} effectively stabilised the CeO_2 against sintering [50]. As a general trend an increase in the amount of added cation decreased the rate of sintering. For the tetravalent cations the following order of rates of sintering is found: $Th^{4+}<Zr^{4+}\ll Si^{4+}$. Presence of associated defects of the type $(Me_{Ce}, Ce_{Ce})'$, where electrons in the reduced cerium cation are associated with the neighbouring foreign cation, was invoked to explain this observation. Higher the electronegativity of the foreign atom, higher the tendency to form such associated defects. Qualitatively such defects should be less mobile than Ce'_{Ce}, accounting for the low rate of sintering. Unfortunately, neither experimental nor calculated evidence has been reported so far for such type of defects. Also, it seems reasonable that the ability of the foreign cation to share electrons with the $Ce_{Ce}{}'$ should preferably be related to the fourth ionisation energy, which, however, does not follow the observed order (Th 28.8 eV, Zr 34.34 eV, Si 45.41 eV). Significantly, both magnetic susceptibility and XANES measurements indicated that reduction of CeO_2–ZrO_2 leads to formation of reduced Ce^{3+} sites ($Ce_{Ce}{}'$) and no evidence for Zr^{4+} accepting electrons was found [66,67]. This is in agreement with the higher fourth ionisation energy for cerium (36.72 eV) compared to zirconium. In our view, further work is needed before the general validity of the authors model [50] can be assessed. In fact, although the authors claimed out the structural homogeneity of their solid solutions [85], it is worth noting that all the samples were prepared by an incipient wetness method, followed by a calcination at 723 K for 4 h. In the presence of the relatively large average particle diameter (13.7 nm) and the mild calcination conditions, it cannot be excluded that the observed phenomena could be related simply to the higher ability of small cations compared to large ones of migrating into the CeO_2 lattice and form a solid solution.

Table 3
Effect of tri-valent dopants on the stabilisation of CeO_2 surface area after high temperature calcination [86]

Dopant (mol%)	BET surface area ($m^2\ g^{-1}$) after 1 h calcination at	
	813 K	1253 K
–	80	5
La_2O_3 (5%)	84	33
Nd_2O_3 (5%)	80	26
Y_2O_3 (5%)	92	26
Al_2O_3 (5%)	88	11

Thermal stabilisation of CeO_2 surface area was observed also in mixed oxides prepared by co-precipitation [86]. Remarkably, all the dopant whose radii are larger than that of Ce^{4+}, e.g. La, Nd, and Y, significantly stabilise CeO_2 with respect to high temperature calcination (Table 3). No evidence for separation of the added oxide was found by XRD suggesting that solid solutions were formed. Notably, XPS measurements carried out on La/CeO_2 calcined at 813 and 1253 K showed La/Ce ratios, respectively, of 0.19 and 0.25 indicating that the calcination induced a surface enrichment in the La/CeO_2 mixed oxide with respect to the bulk value (0.11). Remarkably, in an impregnated sample the La/Ce (La/Ce=0.25 in fresh sample) was as high as 0.75 after calcination at 1275 K. A similar surface enrichment was observed for the Nd/CeO_2. It appears that the common mechanism of the stabilisation of surface area with these tri-valent dopants is a surface M^{3+} enrichment that impedes ceria crystallite growth under oxidising conditions [86,87]. Segregation at the surface of low-valent cations together with oxygen vacancies is energetically favoured and may represent the driving force for this surface area stabilisation [88].

The effectiveness of high ZrO_2 content (>10 mol%) on the surface area stability of CeO_2 was also reported [89,90]. Generally speaking, it has been reported for commercial products that an increase of ZrO_2 increases the surface area stability up to approximately 60 mol%. At higher ZrO_2 contents, the surface area is constant (Fig. 5). At variance, the OSC appears maximum for the intermediate ZrO_2 contents (25–50 mol%). A rationale for this behaviour cannot be

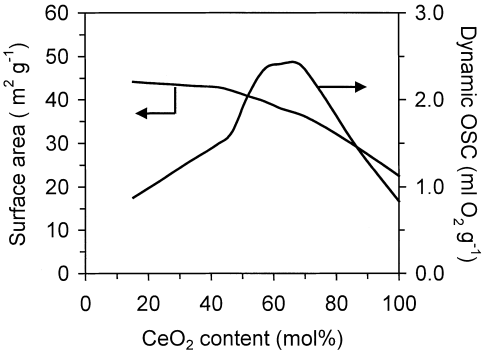

Fig. 5. Thermal stability and OSC at 673 K of "state-of-the-art" CeO_2–ZrO_2 mixed oxides after ageing at 1173 K for 6 h under air atmosphere [90].

given at present, due to a number of reasons. In fact, as discussed above, formation of a homogeneous solid solution over the whole range of composition by using a single optimised process appears unreliable. Accordingly, the authors claimed that homogeneous solid solutions were detected for ZrO_2 molar contents up to 50 mol% [90].

Another important point is that the intrinsic effect of ZrO_2 on the CeO_2 surface area stability, e.g. effects which can be related simply to a compositional change, cannot be detected unless the samples are prepared by a single synthesis method, giving common textural and morphological properties. It is well known that, surface areas, particle morphology and even the phase nature of ZrO_2 are strongly affected by the synthesis conditions [43,45,91]. In fact, by using a high-energy ball milling method for the synthesis of $Ce_xZr_{1-x}O_2$ mixed oxides (x=1, 0.8, 0.5, 0.2, 0) [92], it was observed that the surface area increased with CeO_2 content reaching a maximum for x=0.8, which is exactly the opposite of the trend reported in Fig. 5.

An important factor for the stabilisation of the surface area is the homogeneity of the CeO_2–ZrO_2 mixed oxide. In a comparative study of co-precipitated and impregnated–precipitated CeO_2 (26 mol%)–ZrO_2 aerogels were prepared and characterised [79]. XRD patterns showed traces of m-ZrO_2 in the latter sample while a homogeneous solid solution was formed in the former case. The sintering behaviour was investigated and surface areas of, respectively, 39 and 12 $m^2 g^{-1}$ were measured after calcination at 1223 K. Both samples sintered to a similar particle size (12–14 nm), however, as evidenced by SEM and TEM, the particles remained disperse and relatively separated in the homogeneous solid solution. In contrast, the particles were severely agglomerated in the precipitated–impregnated sample, indicating a different type of sintering behaviour. Surface enrichment in ceria was detected by XPS in the non-homogeneous sample, suggesting that its presence is responsible for the easy particle agglomeration.

The effect of synthesis conditions of the surface area stability of the CeO_2–ZrO_2 mixed oxides was recently addressed by Terribile et al. [93]. They compared the surface areas of samples prepared by the conventional co-precipitation route with those prepared by carrying out the synthesis in the presence of surfactants. As shown in Fig. 6, remarkably high surface areas were obtained by the surfactant route, which persisted after calcination. This effect seems to be ascribed to the presence of an initial surface area, rather than to a modification of the sintering mechanism. Both the co-precipitated and surfactant route samples show indeed comparable % of loss of surface area upon calcination (Fig. 6).

In summary, the efficiency of ZrO_2 to improve the thermal stability of the CeO_2 is now well established but the intrinsic role of ZrO_2 in determining these improved properties is far from being understood. Systematic studies on well-defined materials are necessary to elucidate this important point.

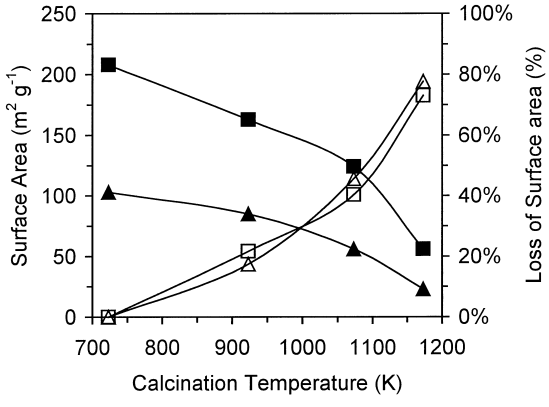

Fig. 6. Surface areas (filled symbols) and % of loss of surface area (open symbols) upon calcination at 773–1173 K of surfactant route (■, □) and co-precipitated (▲, △) CeO_2–ZrO_2 mixed oxides [93].

Thermal stability of CeO_2–ZrO_2 mixed oxides supported on Al_2O_3 has been investigated by researchers from Ford [65]. Samples of the type $Ce_xZr_{1-x}O_2/Al_2O_3$ (x=0.92, 0.81, 0.65, 0.49 and 0) with nominal loading of the mixed oxide ranging from 18 to 44 wt% have been prepared by wet impregnation of Al_2O_3 with ceria and zirconia-containing nitrate solution to the incipient wetness. After calcination at 673 K for 4 h, formation of CeO_2–ZrO_2 solid solutions supported on Al_2O_3 was detected by XRD. However, all the observed lattice parameters were systematically higher than the reference JPCDS[3] files. This suggested that by this methodology, the insertion of ZrO_2 into the CeO_2 lattice was only partially accomplished, the rest of ZrO_2 being anchored to the Al_2O_3 support in a highly dispersed form. Accordingly, no evidence for crystalline ZrO_2 is found in the XRD pattern of the fresh ZrO_2-only/Al_2O_3 sample (Fig. 7).

The favourable effects of ZrO_2 addition to CeO_2 were observed after ageing under both hydrothermal and reducing conditions: After hydrothermal aging the particle size of approx. 27 nm was found for CeO_2/Al_2O_3 which decreased below 20 nm for the ZrO_2-containing samples. As detected by TEM and XRD in the aged samples, the CeO_2–ZrO_2 particle size decreased as the ZrO_2 content increased from 0 to 50 mol%. This is an interesting result since the CeO_2–ZrO_2 loading was increased from 26 to 44 wt% in these samples. The favourable effect of Al_2O_3 on CeO_2 dispersion should be less effective on increasing the content of the supported phase. There is, however, a possible drawback of using high ZrO_2 contents shown in Fig. 7. This splitting of the (1 1 1) peak indicates that a partial separation of a tetragonal $Ce_xZr_{1-x}O_2$ phase occurred in the $Ce_{0.49}Zr_{0.51}O_2$ (44 wt%)/Al_2O_3. This phase separation is consistent with the limited mutual solubility of CeO_2–ZrO_2 system [32] and may represent a drawback for the development of thermally stable CeO_2–ZrO_2-based TWCs since the modification of the catalysts upon ageing is undesirable. At present, however, it cannot be excluded that the phase separation can be attributed to an intrinsic sample non-homogeneity due to the synthesis method. In fact, the particle sizes as determined by XRD were systematically higher than those

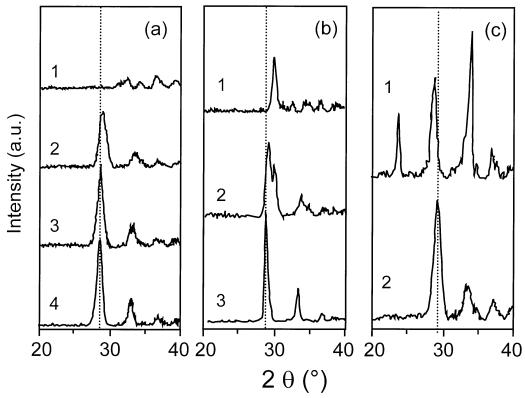

Fig. 7. XRD patterns of fresh (a), steamed (b) (24 h, 10% H_2O, 1273 K) and (c) reduced (H_2/Ar 8.85%, 1173 K) $Ce_xZr_{1-x}O_2$ mixed oxides supported on Al_2O_3: (1) ZrO_2 (18 wt%)/Al_2O_3, (2) $Ce_{0.49}Zr_{0.51}O_2$ (44 wt%)/Al_2O_3, (3) $Ce_{0.81}Zr_{0.19}O_2$ (28 wt%)/Al_2O_3, and (4) CeO_2 (26 wt%)/Al_2O_3 [65].

measured by HRTEM, suggesting the presence of compositional fluctuation, which lead to apparent XRD peak broadening. Statistically, the higher Zr loading, the greater opportunity for compositional fluctuation. This interpretation seems be substantiated by the XRD patterns reported in Fig. 8.

Both the as prepared samples (Fig. 8) do not show evidence for the presence of a CeO_2–ZrO_2 mixed oxide due to the high dispersion of the supported phase. On increasing progressively the calcination temperature, a single phase product is observed when the synthesis is optimised to produce a solid solution. A tetragonal and a cubic phase are observed in the case of the co-impregnated product. No significant evidence for change of relative intensities of the (1 1 1) reflection is observed in the latter case suggesting that the observed modifications of the XRD patterns can be associated to a parallel growth of particle size of the two phases rather than to a phase separation induced by the calcination. This result points out that an extremely careful characterisation of the as synthesised products is necessary before the effects of the thermal treatments of the phase stability can be assessed.

There is another interesting observation reported in Fig. 7(C). It appears that the presence of ZrO_2 inhibits the undesirable interaction of CeO_2 with Al_2O_3 preventing the deactivation of the Ce^{4+}/Ce^{3+} redox couple due to formation of $CeAlO_3$ [95]. The latter

[3]Joint Committees on Powder Diffraction Standards.

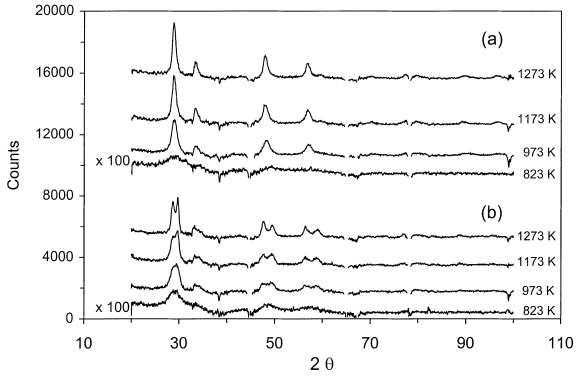

Fig. 8. Effect of calcination (5 h at the indicated temperature) on powder XRD patterns of $Ce_{0.6}Zr_{0.4}O_2/Al_2O_3$ samples prepared by different synthetic methods. XRD patterns are subtracted from the Al_2O_3 contribution: (a) proprietary sample; (b) co-impregnated sample [94].

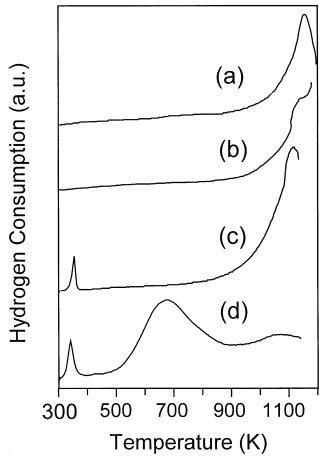

Fig. 9. The temperature programmed reduction (TPR) profiles of LSA samples: (a) CeO_2, (b) $Ce_{0.6}Zr_{0.4}O_2$, (c) 0.5 wt% Rh/CeO_2, and (d) 0.5 wt% $Rh/Ce_{0.6}Zr_{0.4}O_2$ [66].

species is clearly detected in the CeO_2/Al_2O_3 after reduction at 1173 K.

2.1.2. *Redox properties: textural and structural dependence*

The evidence for the importance of ZrO_2 in modifying the redox behaviour of CeO_2 was first reported in open literature by Japanese authors [60,69,80]. Formation of CeO_2–ZrO_2 mixed oxides by a co-precipitation method decreased the temperature of the reduction in the bulk from 1100 to about 900 K [69]. This was attributed to the high oxygen mobility in the bulk of the oxide induced by the insertion of ZrO_2 into the CeO_2 lattice. Shortly later we reported an unusual observation [66] that the reduction occurred at very mild temperatures (600–700 K) in the bulk of Rh-loaded CeO_2–ZrO_2 solid solutions despite the fact that these systems were prepared by a solid state synthesis. This synthesis, which consists of firing a mixture of oxides at 1873 K produces dense ceramic materials which features a very low surface area (LSA, $\approx 1\ m^2\ g^{-1}$). The ability of the sintered Rh/CeO_2–ZrO_2 solid solutions to undergo reduction at mild temperatures is exemplified in Fig. 9, which reports the TPR profiles for Rh-loaded and metal-free $Ce_{0.6}Zr_{0.4}O_2$. The comparison of the TPR traces of the Rh-loaded CeO_2 and $Ce_{0.6}Zr_{0.4}O_2$ immediately reveals that there is a strong reduction peak at ca. 700 K in the ZrO_2-containing catalyst, which is missing in the other systems. This feature is attributed to the promotion of the reduction in the bulk of the mixed oxide, since surface effects can be excluded in these samples.

These initial studies have stimulated interest on investigating the effects of doping of CeO_2 with ZrO_2 and other related materials to promote the CeO_2 redox properties [58,67,68,86,96–99]. As earlier recognised in [100,101], structural doping of CeO_2 may provide an efficient route to enhance the oxygen storage and hence the catalytic activity under transient conditions. In these early studies, the idea was that insertion of a low-valent ion, such as the tri-valent La or Gd should enhance the oxygen anion mobility in the CeO_2, increasing the OSC of these materials. According to Cho [101], two types of oxygen vacancies are created in the doped ceria: intrinsic and extrinsic. The former is due to the reduction of Ce^{4+} according to the following reaction:

$$2Ce_{Ce}^{x} + O_O \rightarrow 2Ce'_{Ce} + V_O^{\cdot\cdot} + \tfrac{1}{2}O_2$$

while the latter is created by the insertion of the bi- or tri-valent cation according to the following reactions:

$$MO \overset{CeO_2}{\rightarrow} M'_{Ce} + V_O^{\cdot\cdot} + \tfrac{1}{2}O_2$$

$$M_2O_3 \overset{CeO_2}{\rightarrow} 2M'_{Ce} + 2O_O^{x} + V_O^{\cdot\cdot} + \tfrac{1}{2}O_2$$

Both of these vacancies were believed to provide a practical way to increase the OSC of CeO_2. This is true

if the oxygen anion mobility is considered. Solid CeO_2-based electrolytes show indeed an increased ionic mobility when doped with low-valent cations [102]. On the contrary, the doping may lead to a decrease of the total-OSC. In fact, the overall degree of reduction of CeO_2 is generally limited by some kind of a non-stoichiometric compound. This means that starting from an oxygen deficient system of the type $M_xCe_{1-x}O_{2-x/2}$ less oxygen vacancies are needed to achieve a certain degree of non-stoichiometry compared to a fully oxidised CeO_2.

The interpretation of the reduction features reported in Fig. 9 seems straightforward [66,67]:

1. ZrO_2 promotes the reduction in the bulk of the mixed oxide;
2. to observe this effect, the presence of the noble metal is necessary, which activates H_2 and spills it over the support favouring its reduction.

A detailed structural characterisation of these solid solutions by XRD, Raman and EXAFS techniques [67,103] suggested fundamental redox properties – structural relationships in these ceramic type CeO_2–ZrO_2 solid solutions. Insertion of progressively increasing amount of ZrO_2 into the CeO_2 fluorite lattice up to 50 mol% is responsible for:

1. a decrease of lattice parameter, due to the smaller Zr^{4+} (0.80 Å) compared to Ce^{4+} (0.97 Å) [67];
2. an increase of the channel diameter for the oxygen migration in the lattice;
3. a progressive increase of structural defects;
4. a decrease of the number of the nearest neighbours oxygens around the Zr^{4+} from 8 to 6 in the $Ce_{0.5}Zr_{0.5}O_2$;
5. no variation of the Ce–O co-ordination sphere except for some shortening of the Ce–O bond length consistent with the contraction of the cell parameter.

Given the stoichiometry of the CeO_2–ZrO_2 solid solutions, the apparent decrease of the co-ordination number was attributed to a high structural disorder of the ''missed'' oxygens induced by to the insertion of ZrO_2 [103]. These two ''invisible'' oxygen are located at a Zr–O bond distance higher than 2.7 Å suggesting a large oxygen lability.

A different situation is found in the tetragonal region, e.g. for $ZrO_2 \geq 50$ mol%. Here ZrO_2 becomes the dominant factor of the phase nature. The Zr–O bonds now assume the typical geometry of tetragonal zirconias, e.g. four short and four long Zr–O bonds, indicating that the structural disorder found in the cubic phase is no longer present. Consistently, the amount of lattice defects remains constant in the tetragonal region [67]. The progressive tetragonalisation with increasing amount of ZrO_2 provides now an effective route for the release of the lattice stress induced by the ZrO_2 insertion resulting in a lower oxygen mobility. All these results clearly point out that the oxygen mobility in the lattice is a key factor in determining the facility of the Ce^{4+} reduction in the bulk of these highly sintered CeO_2–ZrO_2 solid solutions.

Whether these results can be extended to the redox properties of the high surface area systems remains, however, to be ascertained. In fact, the dependence of the reduction behaviour of the CeO_2–ZrO_2 mixed oxides upon textural properties is rather intriguing. For example, for the $Ce_{0.5}Zr_{0.5}O_2$ composition the following TPR behaviour was observed: a single peak at 950 K [58] and two peaks at 880 and 1000 K for surface areas of, respectively, 22 and 64 $m^2\ g^{-1}$) [36]. In another investigation two peaks at 800 and 1000 K were found [69]. In contrast, the ultimate degree of reduction is approximately constant, e.g. a composition of $Ce_{0.5}Zr_{0.5}O_{1.85}$ is obtained after a reduction at 1273 K [36,58]. Further, the treatment under H_2 in the TPR leads to a strong sintering of the mixed oxides and the surface area drops to or below 10 $m^2\ g^{-1}$, which as shown in Fig. 10, leads to a decrease in the reduction temperature compared to the fresh, high surface sample (HSA) [36,76]. This effect is even more remarkable in the presence of the supported noble metal where the reduction of the aged samples occurs at a temperature as low as 440 K for Rh. Clearly, both textural and structural factors govern the redox behaviour of these mixed oxides. Also worth noting is that conventional characterisation methods may fail in determining the presence of microdomains in the mixed oxide which in turn affect the redox behaviour [75,104].

A possible interpretation of the unusual redox behaviour reported in Fig. 10 was given by the comparison of the Raman spectra of the fresh and aged $Ce_{0.5}Zr_{0.5}O_2$ (HSA). Both the fresh metal-free and Rh-loaded $Ce_{0.5}Zr_{0.5}O_2$ (HSA) featured a strong T_{2g} band

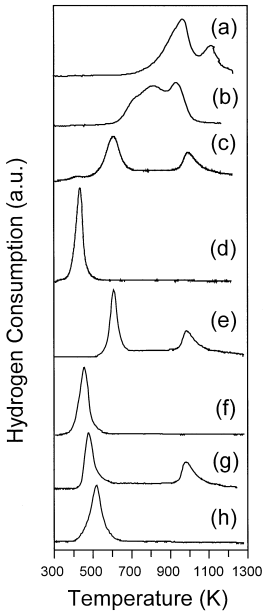

Fig. 10. TPR profiles of fresh and recycled/oxidised at 700 K samples: $Ce_{0.5}Zr_{0.5}O_2$ (a) fresh, (b) recycled; $Rh/Ce_{0.5}Zr_{0.5}O_2$ (c) fresh, (d) recycled; $Pt/Ce_{0.5}Zr_{0.5}O_2$ (e) fresh, (f) recycled; $Pd/Ce_{0.5}Zr_{0.5}O_2$ (g) fresh, (h) recycled [105–107].

at 465 cm^{-1} attributed to a total symmetric M–O (M=Zr, Ce) stretching mode whose intensity strongly decreased upon ageing in TPR/oxidation processes. This was taken as an indication of a progressive breaking of the symmetry of the M–O bond leading to an oxygen sublattice as observed in the $Ce_{0.5}Zr_{0.5}O_2$ (LSA). This interpretation was further substantiated by the TPR profiles of the noble metal-loaded HSA $Ce_{0.5}Zr_{0.5}O_2$. In the presence of the noble metal, hydrogen activation is unlikely to rate limit the reduction process. Consistently, spilling of H_2 to the support surface is responsible for the shift of the surface reduction from 770 to 400–450 K in the HSA CeO_2 in the presence of the noble metal [108] (Fig. 1). Accordingly, the reduction peak observed at 880 K in the fresh $Ce_{0.5}Zr_{0.5}O_2$ (HSA) shifts to 500–700 K in the presence of Rh, Pt or Pd, leaving the peak at 1100 K unaffected. The sintering occurring in the TPR modifies the oxygen sublattice, which increases the oxygen mobility in the bulk and shifts the whole reduction process to low temperatures.

The importance of the oxygen migration in controlling the rate of CeO_2–ZrO_2 reduction was recently questioned by Hori et al. [109]. In fact, by measuring the rate of CO oxidation carried out by pulsing CO over the CeO_2–ZrO_2 at 873 K, the calculated flux of oxygen from bulk of the oxide to the surface was reported several order of magnitude higher than that experimentally measured. Unfortunately, there is a strong variability in the values of oxygen diffusion coefficients reported in the literature and it turns out that, e.g. upon applying those reported in [110,111] surface reaction results faster than oxygen migration in the bulk.

The redox behaviour of ternary CeO_2–ZrO_2 systems using tri-valent oxides as dopants was also investigated [75,112]. Ga^{3+}, Y^{3+} and La^{3+} were inserted into the $Ce_{0.6}Zr_{0.4}O_2$ lattice [75]. Of these cations, the ionic radius of Y^{3+} (1.1015 Å) is very close to the critical one, Ga^{3+} (0.62 Å) and La^{3+} (1.18 Å) are, respectively, undersized and oversized ones. Conventionally, the critical radius is defined as the radius which gives no expansion to the lattice upon substitution. Remarkable modifications of the TPR profiles were found, which can be summarised as follows:

1. an appropriate amount (2.5–5.0 mol%) of the trivalent dopants is necessary to achieve a significant improvement of the reduction;
2. among the cations investigated, the one whose ionic radius is closest to the critical radius of the $Ce_{0.6}Zr_{0.4}O_2$ is the most effective in promoting the reducibility at a low temperature;
3. the OSC measured after a low temperature reduction is improved by about 30% compared to the undoped sample. In contrast the total-OSC measured after a reduction at 1273 K is less affected (see above).

A remarkable point in all these investigations is that redox ageing often leads to improved TPR behaviour at moderate temperatures (compare Fig. 10), suggesting a high thermal stability of the OSC in the CeO_2–ZrO_2 mixed oxides. Accordingly, Permana et al. [20] found that a NM/CeO_2–ZrO_2/Al_2O_3 catalyst is far less de-activated by thermal ageing with respect to NM/CeO_2–ZrO_2/Al_2O_3 (Fig. 11). The comparison with data reported in Fig. 2 clearly shows the superior thermal stability of the ZrO_2-containing catalysts. The lack of OSC deactivation appears in agreement with the results of the investigation of the redox behaviour.

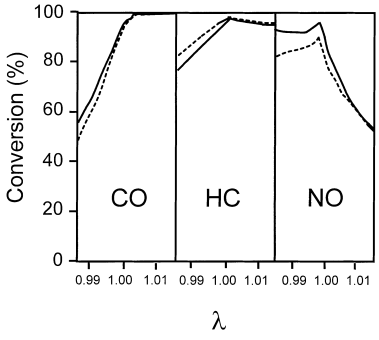

Fig. 11. Effects of thermal ageing at 1173 K on CO, HC and NO_x conversion efficiency (%) for $NM/Ce_{0.75}Zr_{0.25}O_2/Al_2O_3$ during cycled sweep test; (———) fresh, (- - -) aged, GHSV 65 000 h^{-1}, reaction temperature 823 K [20].

3. Conclusions

As discussed above, CeO_2–ZrO_2 mixed oxides represent an important improvement of the TWC technology since the advent of the CeO_2 in the exhaust control in the early 1980s. In particular thermal stability of both surface area and OSC are positively affected by the insertion of ZrO_2 in the catalyst formulation. Despite increasing evidence, a fundamental knowledge of the role of ZrO_2 is still lacking. The variability of the redox properties seems to be related to the synthesis conditions and hence to sample homogeneity [75]. The understanding of how the homogeneity/dishomogeneity of the mixed oxide influences the catalytic activity would represent an important breakthrough point for development of new generation TWCs.

Acknowledgements

University of Trieste, the Ministero dell'Ambiente (Roma), contract n. DG 164/SCOC/97, CNR (Roma) Programmi Finalizzati "Materiali Speciali per Tecnologie Avanzate II, Contract n. 97.00896.34 are gratefully acknowledged for financial support.

References

[1] K.C. Taylor, in: J.R. Anderson, M. Boudart (Eds.), Catalysis-Science and Technology, Chapter 2, Springer, Berlin, 1984.
[2] K.C. Taylor, Catal. Rev.-Sci. Eng. 35 (1993) 457.
[3] P. Degobert, Automobiles and Pollution, Society of Automotive Engineers, Inc., Warrendale, PA, USA, 1995.
[4] J.T. Kummer, J. Phys. Chem. 90 (1986) 4747.
[5] R.W. McCabe, J.M. Kisenyi, Chem. Ind. London (1995) 605.
[6] M. Prigent, Bulletin Des Societes Chimiques Belges 105 (1996) 139.
[7] M. Shelef, G.W. Graham, Catal. Rev.-Sci. Eng. 36 (1994) 433.
[8] A. Trovarelli, Catal. Rev.-Sci. Eng. 38 (1996) 439.
[9] R.M. Heck, R.J. Farrauto, Catalytic Air Pollution Control. Comercial Technology, Van Nostrand Reinhold, New York, 1995.
[10] A. Frennet, J.M. Bastin (Eds.), Catalysis and Automotive Pollution Control III, Elsevier, Amsterdam, 1995.
[11] N. Kruse, A. Frennet, J.M. Bastin (Eds.), Catalysis and Automotive Pollution Control IV, Elsevier, Amsterdam, 1998.
[12] Zirconium in Emission Control, Society of Automotive Engineers, Inc., Warrendale, PA, 1997.
[13] H.C. Yao, Y. Yu, J. Catal. 86 (1984) 254.
[14] M.F.L. Johnson, J. Mooi, J. Catal. 103 (1987) 502.
[15] S. Bernal, J.J. Calvino, G.A. Cifredo, J.M. Rodriguez-Izquierdo, V. Perrichon, A. Laachir, J. Chem. Soc., Chem. Commun. (1992) 460.
[16] A. Trovarelli, G. Dolcetti, C. de Leitenburg, J. Kaspar, P. Finetti, A. Santoni, J. Chem. Soc., Faraday Trans. 88 (1992) 1311.
[17] S. Bernal, J.J. Calvino, G.A. Cifredo, A. Laachir, V. Perrichon, J.M. Herrmann, Langmuir 10 (1994) 717.
[18] V. Perrichon, A. Laachir, S. Abouarnadasse, O. Touret, G. Blanchard, Appl. Catal. A 129 (1995) 69.
[19] P. Fornasiero, J. Kaspar, M. Graziani, J. Catal. 167 (1997) 576.
[20] H. Permana, D.N. Belton, M. Rahmoeller, S.J. Schmieg, C.E. Hori, A. Brenner, K.Y.S. Ng, SAE 970462 (1997).
[21] European Patent EP 337 809 (1989), Appl.18/10/1989.
[22] M. Yashima, T. Hirose, S. Katano, Y. Suzuki, M. Kakihana, M. Yoshimura, Phys. Rev. B 51 (1995) 8018.
[23] M. Yashima, T. Mitsuhashi, H. Takashina, M. Kakihana, T. Ikegami, M. Yoshimura, J. Am. Ceram. Soc. 78 (1995) 2225.
[24] Y. Du, M. Yashima, T. Koura, M. Kakihana, M. Yoshimura, Scr. Metall. Mater. 31 (1994) 327.
[25] M. Yashima, H. Arashi, M. Kakihana, M. Yoshimura, J. Am. Ceram. Soc. 77 (1994) 1067.
[26] M. Yashima, H. Takashina, M. Kakihana, M. Yoshimura, J. Am. Ceram. Soc. 77 (1994) 1869.
[27] M. Yashima, K. Morimoto, N. Ishizawa, M. Yoshimura, J. Am. Ceram. Soc. 76 (1993) 2865.
[28] M. Yashima, K. Morimoto, N. Ishizawa, M. Yoshimura, J. Am. Ceram. Soc. 76 (1993) 1745.
[29] A.E. McHale, Phase diagrams for ceramists. Annual 1991, vol. 20, 1991.
[30] S. Meriani, J. De Physique 47 (1986) C1–485.
[31] S. Meriani, Mater. Sci. Eng. A 71 (1985) 365.

[32] E. Tani, M. Yoshimura, S. Somiya, J. Am. Ceram. Soc. 66 (1983) 506.
[33] P. Duran, M. Gonzales, C. Moure, J.R. Jurdo, C. Pascal, J. Mater. Sci. 25 (1990) 5001.
[34] S. Meriani, Mater. Sci. Eng. A 109 (1989) 121.
[35] S. Meriani, Mater. Sci. Eng. 71 (1985) 369.
[36] P. Fornasiero, G. Balducci, R. Di Monte, J. Kaspar, V. Sergo, G. Gubitosa, A. Ferrero, M. Graziani, J. Catal. 164 (1996) 173.
[37] R.C. Garvie, M.F. Goss, J. Mater. Sci. 21 (1986).
[38] R.C. Garvie, J. Phys. Chem. 82 (1978) 218.
[39] R.C. Garvie, J. Phys. Chem. 69 (1965) 1238.
[40] T. Mitsuhasi, M. Ichihara, U. Tatsuke, J. Am. Ceram. Soc. 57 (1974) 97.
[41] J. Livage, K. Doi, C. Mazieres, J. Am. Ceram. Soc. 51 (1968) 349.
[42] K. Tani, M. Yoshimura, S. Somiya, J. Am. Ceram. Soc. 66 (1983) 11.
[43] A. Chatterjee, S.K. Pradhan, A. Datta, M. De, D. Chakravorty, J. Mater. Res. 9 (1994) 263.
[44] B.E. Yoldas, J. Am. Ceram. Soc. (1982) 387.
[45] G. Stefanic, S. Popovic, S. Music, Thermochim. Acta 303 (1997) 31.
[46] V. Longo, D. Minichelli, J. Am. Ceram. Soc. 56 (1973) 1186.
[47] JCPDS (1998) 28–271.
[48] A. Kawabata, S. Hirano, M. Yoshinaka, K. Hirota, O. Yamaguchi, J. Mater. Sci. 31 (1996) 4945.
[49] A.I. Leonov, A.B. Andreeva, E.K. Keler, Izv. Akad. Nauk SSSR, Neorg. Mater. 2 (1966) 137.
[50] M. Pijolat, M. Prin, M. Soustelle, O. Touret, P. Nortier, J. Chem. Soc., Faraday Trans. 91 (1995) 3941.
[51] R.D. Shannon, Acta Cryst. A 32 (1976) 751.
[52] R.D. Shannon, C.T. Prewitt, Acta Cryst. B 26 (1970) 1046.
[53] R.D. Shannon, C.T. Prewitt, Acta Cryst. B 25 (1969) 925.
[54] S.J. Hong, A.V. Virkar, J. Am. Ceram. Soc. 78 (1995) 433.
[55] M. Yashima, N. Ishizawa, M. Yoshimura, J. Am. Ceram. Soc. 75 (1992) 1541.
[56] M. Yashima, N. Ishizawa, M. Yoshimura, J. Am. Ceram. Soc. 75 (1992) 1550.
[57] D.J. Kim, J. Am. Ceram. Soc. 72 (1989) 1415.
[58] C. de Leitenburg, A. Trovarelli, F. Zamar, S. Maschio, G. Dolcetti, J. Llorca, J. Chem. Soc., Chem. Commun. (1995) 2181.
[59] C. de Leitenburg, A. Trovarelli, J. Llorca, F. Cavani, G. Bini, Appl. Catal. A 139 (1996) 161.
[60] M. Ozawa, M. Kimura, A. Isogai, J. Alloys Comp. 193 (1993) 73.
[61] Y. Zhang, S. Andersson, M. Muhammed, Appl. Catal. B 6 (1995) 325.
[62] S.F. Pal'guev, S.I. Alyamosvkii, Z.S. Volchenkova, Russ. J. Inorg. Chem. 4 (1959) 1185.
[63] S. Okikawa, S. Takano, S. Saito, S. Somiya, Bull. Tokyo Inst. Technol. 98 (1970) 53.
[64] P. Duwez, F. Odell, J. Am. Ceram. Soc. 33 (1950) 274.
[65] M.H. Yao, R.J. Baird, F.W. Kunz, T.E. Hoost, J. Catal. 166 (1997) 67.
[66] R. Ranga, J. Kaspar, R. Di Monte, S. Meriani, M. Graziani, Catal. Lett. 24 (1994) 107.
[67] P. Fornasiero, R. Di Monte, R. Ranga, J. Kaspar, S. Meriani, A. Trovarelli, M. Graziani, J. Catal. 151 (1995) 168.
[68] M.Y. Sinev, G.W. Graham, L.P. Haack, M. Shelef, J. Mater. Res. 11 (1996) 1960.
[69] T. Murota, T. Hasegawa, S. Aozasa, H. Matsui, M. Motoyama, J. Alloys Comp. 193 (1993) 298.
[70] Y.L. Chen, M. Qi, D.Z. Yang, K.H. Wu, Mater. Sci. Eng. A 183 (1994) L9.
[71] D. Michel, L. Mazerolles, P. Berthet, E. Gaffet, J. Am. Ceram. Soc. 76 (1993) 2884.
[72] T. Settu, R. Gobinathan, Bull. Chem. Soc. Jpn. 67 (1994) 1999.
[73] T. Settu, R. Gobinathan, J. Eur. Ceram. Soc. 16 (1996) 1309.
[74] M. Yashima, K. Ohtake, M. Kakihana, M. Yoshimura, J. Am. Ceram. Soc. 77 (1994) 2773.
[75] P. Vidmar, P. Fornasiero, J. Kaspar, M. Graziani, J. Catal. 171 (1997) 160.
[76] G. Balducci, P. Fornasiero, R. Di Monte, J. Kaspar, S. Meriani, M. Graziani, Catal. Lett. 33 (1995) 193.
[77] S. Meriani, G. Soraru, in: P. Vicenzini (Ed.), Ceramic Powders, Elsevier, Amsterdam, 1983, pp. 547–554.
[78] V.S. Nagarajan, K.J. Rao, Phil. Mag. A 65 (1992) 771.
[79] Y. Sun, P.A. Sermon, J. Mater. Chem. 6 (1996) 1025.
[80] S. Matsumoto, N. Miyoshi, T. Kanazawa, M. Kimura, M. Ozawa, in: S. Yoshida (Ed.), Catalytic Science and Technology, VCH/Kodansha, Weinheim/Tokyo, 1991, pp. 335–338.
[81] F. Gruy, M. Pijolat, J. Am. Ceram. Soc. 77 (1994) 1537.
[82] M. Pijolat, M. Prin, M. Soustelle, O. Touret, J. Chim. Phys. Phys.-Chim. Biol. 91 (1994) 37.
[83] M. Pijolat, M. Prin, M. Soustelle, P. Nortier, J. Chim. Phys. Phys.-Chim. Biol. 91 (1994) 51.
[84] M. Pijolat, M. Prin, M. Soustelle, O. Touret, P. Nortier, Solid State Ionics 63 64 65 (1993) 781.
[85] M. Prin, Thesis, Ecole Nationale Superieure des Mines, Saint Etiene, France, 1991.
[86] J.E. Kubsch, J.S. Rieck, N.D. Spencer, in: A. Crucg (Ed.), Catalysis and Automotive Pollution Control II, Elsevier, Amsterdam, 1991, pp. 125–138.
[87] P.G. Harrison, D.A. Creaser, B.A. Wolfindale, K.C. Waugh, M.A. Morris, W.C. Mackrodt, in: T.J. Dines, C.H. Rochester, J. Thomson (Eds.), Catalysis and Surface Characterisation, The Royal Socitey of Chemistry, Cambridge, 1996, pp. 76–86.
[88] T.X.T. Sayle, S.C. Parker, C.R.A. Catlow, J. Phys. Chem. 98 (1994) 13625.
[89] A. Trovarelli, C. de Leitenburg, G. Dolcetti, CHEMTECH 27 (1997) 32.
[90] J.P. Cuif, G. Blanchard, O. Touret, A. Seigneurin, M. Marczi, E. Quémeré, SAE 970463 (1997).
[91] G.K. Chuah, S. Jaenicke, Appl. Catal. A 163 (1997) 261.
[92] F. Zamar, A. Trovarelli, C. de Leitenburg, G. Dolcetti, Stud. Surf. Sci. Catal. 101 (1996) 1283.
[93] D. Terribile, A. Trovarelli, J. Llorca, C. de Leitenburg, G. Dolcetti, Catal. Today 43 (1998) 79.

[94] R. Di Monte, J. Kaspar, P. Fornasiero, A. Ferrero, G. Gubitosa, M. Graziani, Stud. Surf. Sci. Catal. 116 (1998) 559.
[95] J.Z. Shyu, W.H. Weber, H.S. Gandhi, J. Phys. Chem. 92 (1988) 4964.
[96] F. Zamar, A. Trovarelli, C. de Leitenburg, G. Dolcetti, J. Chem. Soc. Chem. Commun. (1995) 965.
[97] R.K. Usmen, G.W. Graham, W.L.H. Watkins, R.W. McCabe, Catal. Lett. 30 (1995) 53.
[98] S. Bernal, G. Blanco, G.A. Cifredo, J.A. Perezomil, J.M. Pintado, J.M. Rodriguez-Izquierdo, J. Alloys Comp. 250 (1997) 449.
[99] A.D. Logan, M. Shelef, J. Mater. Res. 9 (1994) 468.
[100] T. Miki, T. Ogawa, M. Haneda, N. Kakuta, A. Ueno, S. Tateishi, S. Matsuura, M. Sato, J. Phys. Chem. 94 (1990) 6464.
[101] B.K. Cho, J. Catal. 131 (1991) 74.
[102] H.L. Tuller, A.S. Nowick, J. Electrochem. Soc. 122 (1975) 255.
[103] G. Vlaic, P. Fornasiero, S. Geremia, J. Kaspar, M. Graziani, J. Catal. 168 (1997) 386.
[104] T. Egami, W. Dmowski, R. Brezny, SAE, 970461 (1997).
[105] G. Balducci, P. Fornasiero, R. Di Monte, J. Kaspar, S. Meriani, M. Graziani, Catal. Lett. 33 (1995) 193.
[106] R. DiMonte, P. Fornasiero, M. Graziani, J. Kaspar, J. Alloys Comp. 277 (1998) 877.
[107] P. Fornasiero, G. Balducci, R. Di Monte, J. Kaspar, V. Sergo, G. Gubitosa, A. Ferrero, M. Graziani, J. Catal. 164 (1996) 173.
[108] B. Harrison, A.F. Diwell, C. Hallett, Plat. Met. Rev. 32 (1988) 73.
[109] C.E. Hori, H. Permana, K.Y.S. Ng, A. Brenner, K. More, K.M. Rahmoeller, D.N. Belton, Appl. Catal. B 16 (1998) 105.
[110] D. Martin, D. Duprez, J. Phys. Chem. 100 (1996) 9429.
[111] R. Taha, D. Martin, S. Kacimi, D. Duprez, Catal. Today 29 (1996) 89.
[112] K. Yamada, H. Tanaka, M. Yamamoto, SAE 970464 (1997).